Journal of Pharmaceutical Analysis 12 (2022) 637–644

Contents lists available at ScienceDirect

Journal of Pharmaceutical Analysis

journal homepage: www.elsevier.com/locate/jpa

Original article

A highly sensitive bio-barcode immunoassay for multi-residue detection of organophosphate pesticides based on fluorescence anti-quenching

Lingyuan Xu [a], Xiuyuan Zhang [a], A.M. Abd El-Aty [b, c], Yuanshang Wang [a], Zhen Cao [a], Huiyan Jia [d], J.-Pablo Salvador [e, f], Ahmet Hacimuftuoglu [c], Xueyan Cui [a], Yudan Zhang [a], Kun Wang [a], Yongxin She [a], Fen Jin [a], Lufei Zheng [a, **], Baima Pujia [g], Jing Wang [a], Maojun Jin [a, h, *], Bruce D. Hammock [h]

[a] Institute of Quality Standard and Testing Technology for Agro-Products, Chinese Academy of Agricultural Sciences, Beijing, 100081, China
[b] Department of Pharmacology, Faculty of Veterinary Medicine, Cairo University, Giza, 12211, Egypt
[c] Department of Medical Pharmacology, Medical Faculty, Ataturk University, Erzurum, 25240, Türkiye
[d] Institute of Livestock and Poultry, Ningbo Academy of Agricultural Sciences, Ningbo, Zhejiang, 315040, China
[e] Nanobiotechnology for Diagnostics Group, Instituto de Química Avanzada de Cataluña, IQAC-CSIC, Barcelona, 08034, Spain
[f] CIBER de Bioingeniería, Biomateriales y Nanomedicina (CIBER-BBN), Madrid, 28029, Spain
[g] Inspection and Testing Center of Agricultural and Livestock Products of Tibet, Department of Agriculture and Rural Affairs of Tibet Autonomous Region, Lhasa, 850000, China
[h] Department of Entomology & Nematology and the UC Davis Comprehensive Cancer Center, University of California, Davis, CA, 95616, USA

ARTICLE INFO

Article history:
Received 12 October 2021
Received in revised form
11 May 2022
Accepted 14 May 2022
Available online 20 May 2022

Keywords:
Organophosphate pesticides
Fluorescence anti-quenching
Gold nanoparticles
DNA-RNA hybridization
DNA oligonucleotides
Ribonuclease H

ABSTRACT

Balancing the risks and benefits of organophosphate pesticides (OPs) on human and environmental health relies partly on their accurate measurement. A highly sensitive fluorescence anti-quenching multi-residue bio-barcode immunoassay was developed to detect OPs (triazophos, parathion, and chlorpyrifos) in apples, turnips, cabbages, and rice. Gold nanoparticles were functionalized with monoclonal antibodies against the tested OPs. DNA oligonucleotides were complementarily hybridized with an RNA fluorescent label for signal amplification. The detection signals were generated by DNA-RNA hybridization and ribonuclease H dissociation of the fluorophore. The resulting fluorescence signal enables multiplexed quantification of triazophos, parathion, and chlorpyrifos residues over the concentration range of 0.01–25, 0.01–50, and 0.1–50 ng/mL with limits of detection of 0.014, 0.011, and 0.126 ng/mL, respectively. The mean recovery ranged between 80.3% and 110.8% with relative standard deviations of 7.3%–17.6%, which correlate well with results obtained by liquid chromatography-tandem mass spectrometry (LC-MS/MS). The proposed bio-barcode immunoassay is stable, reproducible and reliable, and is able to detect low residual levels of multi-residue OPs in agricultural products.

1. Introduction

Organophosphate pesticides (OPs) are among the most widely used insecticides in agricultural production, protecting crops from pest damage and maintaining high and stable production yields. OPs were developed to replace organochlorines; however, many of them are more toxic than the compounds they were meant to replace. Organophosphate residues can reach lakes, rivers, and other water bodies through direct runoff. Therefore, long-term exposure to large quantities of OPs may cause significant harm to ecosystems and human health [1]. Dietary exposure to OPs exceeding the maximum tolerated dose might inhibit acetylcholinesterase activity, causing the accumulation of the neurotransmitter acetylcholine, leading to prolonged overstimulation of cholinergic receptors and causing cholinergic toxicity, such as kinesthesia and respiratory failure [2]. Moreover, the widespread

Peer review under responsibility of Xi'an Jiaotong University.
* Corresponding author. Institute of Quality Standard and Testing Technology for Agro-Products, Chinese Academy of Agricultural Sciences, Beijing, 100081, China.
** Corresponding author.
E-mail addresses: zhenglufei@caas.cn (L. Zheng), jinmaojun@caas.cn (M. Jin).

https://doi.org/10.1016/j.jpha.2022.05.004

use of OPs in the environment may cause soil acidification and compaction, accelerating soil degradation [3]. The bioaccumulation of OPs may exert a tremendous toxic effect on human and animal health [4]. Pesticide residues are receiving much attention in agricultural safety studies. Balancing the risks and benefits of OPs relies partly on their accurate measurement to ensure human and environmental health. Thus, it is essential to develop simple, rapid, sensitive, and precise methods to determine OP residues in different matrices.

So far, various techniques, such as immunoassays, spectroscopy, and chromatography, have been used for the qualitative and quantitative detection of residual OPs. Enzyme-linked immunosorbent assay [5] provides a reliable method for the qualitative and semi-quantitative detection of pesticide residues with simplicity, high selectivity, and reproducibility. Chemiluminescence immunoassay [6] has the advantages of being simple, rapid and safe, and having high sensitivity, short detection time, wide detection range and high sensitivity. Meanwhile, fluorescence immunoassay [7] has the advantages of having high specificity, high sensitivity, a wide range of standard curves, fast analysis, easy preparation of the markers, a long effective use period, and no radioactive contamination. The biosensor method has the advantages of having an economical, simple operation with high analytical accuracy and specificity, but it can only perform semi-quantitative analysis [8]. Chromatographic methods can provide the required high sensitivity and accuracy according to the requirements of government agencies, such as the European Commission, The United States Department of Agriculture, and the Ministry of Agriculture of China. However, in many cases, they cannot detect trace residues due to high detection limits, expensive equipment, and lengthy analysis time [9].

The bio-barcode assay (BCA) was established to simultaneously detect multiple targets in a single run [10]. It is based on the relationship between the DNA barcoding strand and the target protein, which the bio-barcoding technology utilizes to perform multi-residue detection of macromolecular compounds. The corresponding DNA barcode can be designed according to the probe captured by the target. For instance, Stoeva et al. [11] designed nanoparticle probes (NP) to simultaneously detect three tumor protein markers. Additionally, Li et al. [12] designed probes with different types of fluorescence labels and used NP-DNA to detect five DNA sequences and their sources simultaneously. Further, Lin et al. [13] used bimetallic NP for a novel nanoenzyme-based fluorescence amplification method based on biological barcodes that allow simultaneous detection of the RNAs of human immunodeficiency virus and hepatitis C virus. This method has shown excellent detection characteristics. The studies mentioned above have shown that biological barcode detection can be applied to multi-residue detection of macromolecular compounds. In the last few years, the application of colloidal gold and biological barcode signal amplification in immunoassays has attracted much attention due to the unique optical, chemical, catalytic, and electronic properties of colloidal gold [14–17]. Gold nanoparticles (AuNPs) can easily function with biomolecules without affecting their biological activity [18,19]. Using biomolecules (including aptamers [20], amino acids [21], and proteins [22]), electrochemistry [23], colorimetry [24], and fluorescence quenching [25] are the current signal amplification strategies for AuNPs. Bio-barcodes have also been applied in ultra-sensitive immunoassays [26–28].

Fluorescence signals generated during the BCA are due to the activity of RNase H, which explicitly recognizes A-form RNA and B-form DNA, causing the fluorescent group to modify the RNA strand and subjecting it to the inhibitory effect of the quenching group, thus emitting fluorescence at a specific wavelength. A fluorophore is a label with relatively high fluorescence intensity that can also emit fluorescence at a specific wavelength without enhancing or inhibiting the fluorescence of other labels. The particles of the colloidal gold solution are made up of a gold core and a double ion layer around it. The inner layer is an anion layer dominated by tetrachloroaurate ions tightly connected to the surface of the gold core, while H^+ forms the outer ion layer. Colloidal gold is produced by reducing chloroauric acid (HAuCl) with trisodium citrate dehydrate. Biological barcoding uses covalent binding to label single-stranded DNA (ssDNA) chains and antibodies on colloidal gold. However, in labeling ssDNA and antibodies, the instability of charges can easily lead to the irreversible aggregation of gold particles. It has been reported that ultrasensitive immunoassay based on biological barcode nanoparticles and oligonucleotide signal amplification. For instance, Lin et al. [29] developed an ultrasensitive immunoassay for protein biomarkers based on electrochemiluminescent quenching of quantum dots by hemin bio-bar-coded nanoparticle tags. Moreover, Zhang et al. [30] developed a high-sensitivity method for detecting parathion using a competitive biological barcode immunoassay based on bimetallic nano enzyme catalysis. Additionally, our research group has successfully designed various detection and analytical techniques based on colloidal gold and biological barcodes based on the enzyme-linked immunoassay.

Herein, we developed a highly sensitive bio-barcode immunoassay based on fluorescence anti-quenching to simultaneously determine multi-residual levels of OPs, including triazophos, parathion, and chlorpyrifos in apples, turnips, cabbages, and rice. Three colloidal gold nanoprobes were synthesized using different sequences of ssDNA. Each probe hybridized with its complementary sequence and was labeled with a fluorescent moiety. The RNA strands were hybridized and paired, and the fluorescent groups were hydrolyzed by RNase H to generate a fluorescent signal at a specific wavelength. The developed bio-barcode was applied to detect low residual levels of OPs in agricultural products.

2. Experimental

2.1. Materials and reagents

Polyethylene glycol 20000 (PEG 20000), Tris-EDTA (TE) buffer (pH 7.4), ovalbumin (OVA), tris(2-carboxyethyl)phosphine (TCEP), dithiothreitol (DTT), and bovine serum albumin (BSA) were provided by Sigma-Aldrich (St. Louis, MO, USA). Institute of Pesticide and Environmental Toxicology (Zhejiang University, Zhejiang, China) donated antigens (triazophos, parathion, and chlorpyrifos) and their monoclonal antibodies at a concentration of 4.53, 7.57, and 6.31 mg/mL, respectively. Dr. Ehrenstorfer GmbH (Augsburg, Germany) supplied triazophos, parathion, and chlorpyrifos (purity, 98%) and their structural analogs (>95%) standards. RNase H was procured from Takara (Kusatsu, Japan). Shanghai Sangon Biotechnology Co., Ltd. (Shanghai, China) supplied all oligonucleotides. Octadecyltrimethoxysilane (C_{18}, 40–60 μm) and primary-secondary amine (PSA, 40–60 μm) were acquired from Bonna-Agela Technologies (Tianjin, China).

2.2. Design of oligonucleotides

In a previous study, our group developed an immunoassay method for detecting triazophos based on DNA/RNA hybridization using barcoding identification [31]. Herein, we continue to explore the application of the technique for the multi-residue determination of OPs. The design of the oligonucleotide sequence was based on a previous protocol [32]. Table 1 shows three types of synthesized oligonucleotide sequences, three types of 5'-end modified sulfhydryl DNA strands, three types of 3'-end modified quenching

groups (black hole quencher-1, BHQ-1), and three types of 5'-end-modified 6-carboxyfluorescein (6-FAM) RNA strands.

2.3. Preparation of three different oligonucleotide-colloidal gold probes

The preparation of colloidal gold nanoparticles was modified based on a previously reported method [31]. The characterization of nanoparticles and their particle size distribution are shown in Fig. S1. The solution was cooled down to room temperature (25 °C) and then stored at 4 °C for later use. Three tubes with different ssDNA powder samples were centrifuged according to the manufacturer's protocols. Then, 46 μL each of TE buffer and TCEP solution were added, and placed on an oscillator for activation for 3 h. The prepared colloidal gold solution was filtered through a 0.22-μm polyethersulfone membrane (Jintang Experimental Equipment Co., Ltd., Tianjin, China). Then, 1 mL of colloidal gold solution was pipetted into three centrifuge tubes, to which 30 μL of K_2CO_3 solution (pH 9.0) was added. After 15 min, antibodies against triazophos, parathion, and chlorpyrifos, respectively, were added, and the solutions were mixed thoroughly and slowly. One hour later, the corresponding activated oligonucleotide chain solution was added, and the solution was slowly and repeatedly blown to mix thoroughly, and was placed in a 4 °C refrigerator for 16 h. The mixture was equilibrated for approximately 1.5 h at room temperature, then 30% PEG 20000 was added at a final concentration of 0.5% and diluted 20 times. The solution was slowly and repeatedly blown to mix thoroughly. A volume of 0.1 mol/L phosphate-buffered saline (PBS) solution was added every 2 h for 6 times so to a final concentration of 0.01 mol/L. Then, the three solutions were kept at 4 °C for more than 8 h. After the aging process, the solution was placed at room temperature, and then a volume of 10% BSA blocking solution was added to a concentration of 1%. Blocking was done for 1 h. After centrifugation at 13,000 r/min for 15 min, the supernatant was removed, and the residue was redissolved in 400 μL of probe solution and then stored at 4 °C.

2.4. Sample preparation

The samples were prepared based on the modified quick, easy, cheap, effective, rugged, and safe "QuEChERS" method [32]. The tested samples, including apples, turnips, cabbages, and rice, were procured from the local market (Beijing, China). All samples were confirmed to be free from the tested OPs (triazophos, parathion, and chlorpyrifos) using liquid chromatography-tandem mass spectrometry (LC-MS/MS) Briefly, homogenized samples (5 g of sample + 5 mL of water) weighed into a 50 mL centrifuge tube were spiked with three different concentrations of the tested analytes (mixed quasi-solutions) at a concentration of 10, 50, and 100 μg/kg. The mixture was left to stand for at least 30 min. Afterwards, 10 mL of acetonitrile was added and mixed on a Vortex® Genie-2 (Scientific Industries, Bohemia, NY, USA) for 5 min. Next, 4 g of NaCl and 1 g of anhydrous $MgSO_4$ were added and mixed for 5 min to remove water [31]. After that, the tubes were centrifuged at 5,000 r/min for 5 min. Subsequently, 3 mL of supernatant was added to a centrifuge tube containing 150 mg of PSA (40–60 μm), 150 mg of trimethoxy(octadecyl)silane (C_{18}, 40–60 μm), and 450 mg of $MgSO_4$, and centrifuged at 5,000 r/min for 5 min. Finally, the extract was filtered through a 0.22-μm membrane filter (Jin Teng, Tianjin, China) for further detection. Half of the supernatant was analyzed by LC-MS/MS for residue analysis. On the other hand, 100 μL of the solution was concentrated under a stream of nitrogen, then reconstituted with 1 mL of 5% methanol-PBS solution, and assayed using the established bio-barcoding method [33].

Table 1
The sequence of oligonucleotides.

Pesticides	Oligonucleotide	Sequence from 5′ to 3′
Triazophos	ssDNA1	5′-ACTCTATGGG-3′
	6-FAM-RNA1-black hole quencher (BHQ)-1	6-FAM-5′-CCCAUAGAGU-3′-BHQ-1
Parathion	ssDNA2	5′-AACCACAGTG-3′
	Cy3-RNA2-BHQ-1	Cy3-5′-CACUGUGGUU-3′-BHQ-1
Chlorpyrifos	ssDNA3	5′-AGCGTTGTAG-3′
	Cy5-RNA3-BHQ-1	Cy5-5′-CUACAACGCU-3′-BHQ-1

6-FAM, Cy3, and Cy5: fluorescent groups; BHQ-1: fluorescence burst group; FAM: 5'-end-modified 6-carboxyfluorescein; BHQ: 3'-end modified quenching groups; Cy3: *N,N'*-(dipropyl)-tetramethylindocarbocyanine (Cy3)-CACUGUGGUU-BHQ1; Cy5: *N,N'*-(dipropyl)-tetramethylindodicarbocyanine.

2.5. Detection of multi-residual OP levels using a bio-barcode amplification strategy

The detection procedure for OPs (triazophos, parathion, and chlorpyrifos) was as follows: A volume of 100 μL (per well) of triazophos OVA-hapten, parathion OVA-hapten, and chlorpyrifos OVA-hapten at a dilution of 16,000, 8,000, and 8,000 times in 0.01 mol/L PBS solution was added into a 96-MicroWell™ black plate and then incubated at 4 °C overnight. Subsequently, the coated plate was washed with PBST (0.01 mol/L PBS, 0.05% Tween-20, 300 μL for thrice), and blocking buffer (300 μL, 1% BSA in 0.01 mol/L PBS) was added and incubated at 37 °C for 2 h. After blocking, the plate was washed three times with PBST. The probe solutions (for triazophos, parathion, and chlorpyrifos; 50 μL, diluted with 5% methanol-PBS or sample extract) and ssDNA were mixed. AuNPs-monoclonal antibodies (mAbs) complex (50 μL, diluted) was added to 0.01 mol/L PBS solution and incubated at 37 °C for 1 h. Then, the mixture was washed three times with PBST to remove the unbound mixed probe and ssDNA-AuNPs-mAbs complex. The ssDNA-AuNPs-mAbs complex coated on the plate was used in the subsequent reaction. Then, 100 μL of RNase H reaction solution (Tris-HCl buffer, pH 7.5), consisting of 10 mmol/L DTT, 6 mmol/L $MgCl_2$, 0.1 μmol/L RNA probes (FAM-CCCAUAGAGU-BHQ1, *N,N'*-(dipropyl)-tetramethylindocarbocyanine (Cy3)-CACUGUGGUU-

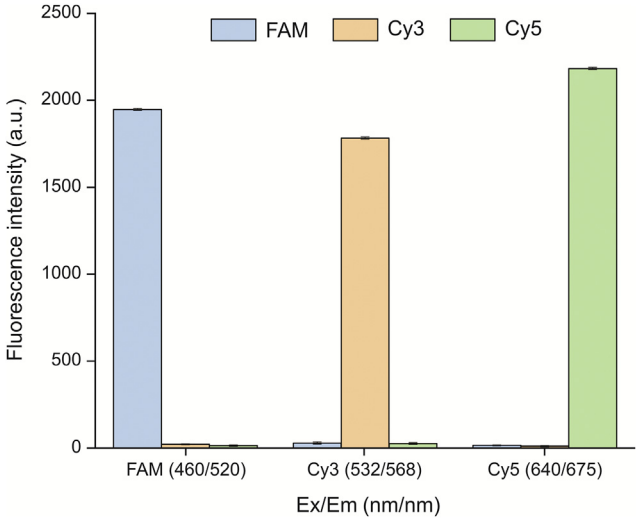

Fig. 1. Fluorescence intensity and interaction between three different fluorophore labels. FAM: 6-carboxyfluorescein; Cy3: *N,N'*-(dipropyl)-tetramethylindocarbocyanine (Cy3)-CACUGUGGUU-BHQ1; Cy5: *N,N'*-(dipropyl)-tetramethylindodicarbocyanine.

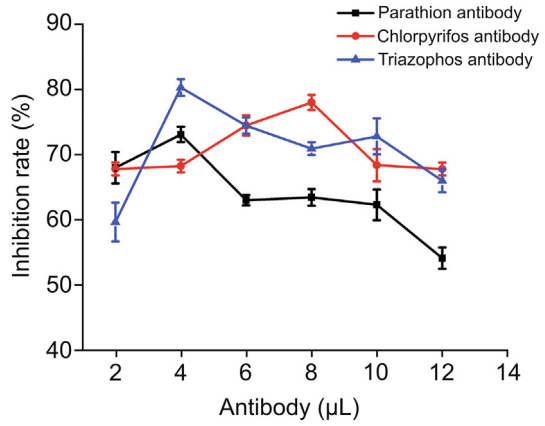

Fig. 2. Optimization of antibodies against the tested organophosphate pesticides.

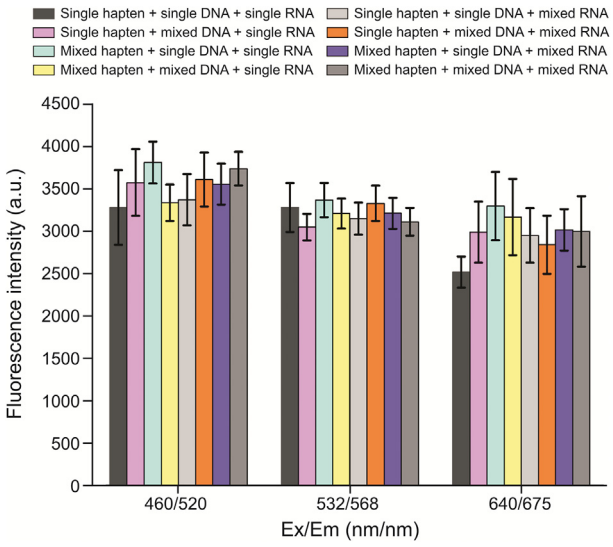

Fig. 3. Cross-reactivity of the assay system.

BHQ1, and *N,N'*-(dipropyl)-tetramethylindodicarbocyanine (Cy5)-CUACAACGCU-BHQ1), and 6 U of ribonuclease H (RNase H) (Takara, Kusatsu, Japan) were added to the system to generate a fluorescent signal. The reaction was carried out at 37 °C for 90 min. Infinite M200 PRO microplate reader (TECAN, Männedorf, Switzerland) was used for detection. We investigated FAM, Cy3, and Cy5 as fluorescent labels and measured their fluorescent signals at specific wavelengths. The fluorescence intensity selected for detection was Ex 460 nm/Em 520 nm, Ex 532 nm/Em 568 nm, and Ex 640 nm/Em 675 nm.

2.6. Spiked recovery experiment

To evaluate the feasibility of the developed method, the samples, including apples, cabbages, radishes, and rice, were secured from a local farmer's market. According to GB 2763-2021, the maximum residue limits (MRLs) of triazophos and chlorpyrifos is 50 μg/kg. In contrast, the MRL for parathion is 10 μg/kg for all vegetables. The samples were tested using LC-MS/MS to ensure they were free from the tested analytes. The conditions for LC-MS/MS are shown in the Supplementary data, and relevant MS parameters of the three pesticides are shown in Table S1. The samples were processed as described in Section 2.4. Homogenized samples were spiked with three different concentrations of the tested analytes (mixed quasi-solutions of triazophos, parathion, and chlorpyrifos) at 10, 50, and 100 μg/kg.

2.7. Statistical analyses

OriginPro 8.5 for Windows was used for data analysis. Each experimental data obtained throughout the study was replicated at least three times. Fluorescence intensity is calculated using the following equation:

$$F_i = \frac{F_{max} - F_x}{F_{max} - F_0} \times 100\%$$

Where F_i represents the inhibition rate of fluorescence intensity, F_{max} represents the maximum fluorescence intensity (the reaction system without adding triazophos, parathion, or chlorpyrifos), F_x is the fluorescence intensity related to the concentration of the tested analytes (triazophos, parathion, and chlorpyrifos), and F_0 is the fluorescence intensity value of blank wells. The limit of detection (LOD) was determined as the concentration of the tested analyte that produced 10% inhibition of the maximum fluorescence.

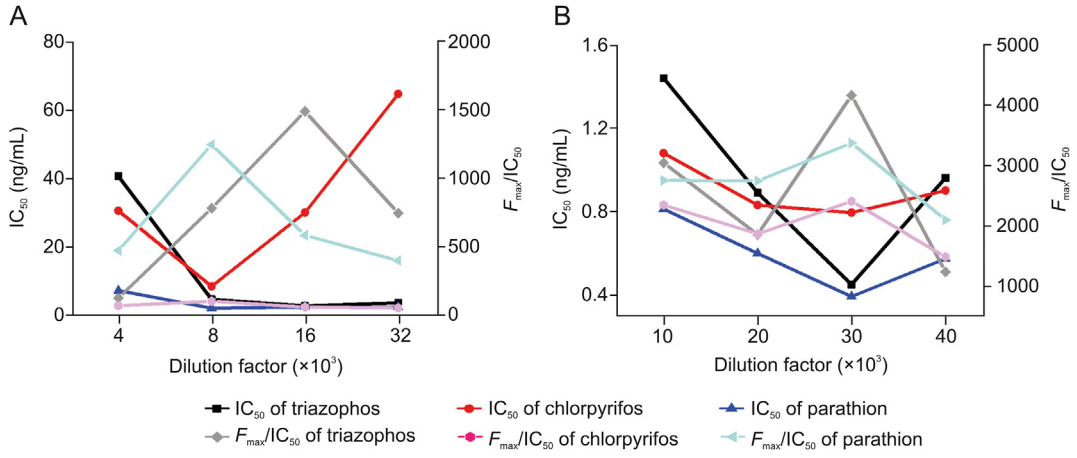

Fig. 4. Optimizing the immunoreagent dilution of (A) ovalbumin (OVA)-haptens and (B) the ssDNA-gold nanoparticles (AuNPs)-monoclonal antibodies (mAbs) complex.

Table 2
The parameters of developed calibration curves of triazophos, parathion, and chlorpyrifos.

Pesticides	Linear equation	Correlation coefficient	Linear range (ng/mL)	IC_{50} (ng/mL)	LOD (ng/mL)
Triazophos	$y = 22.277x + 51.347$	0.977	0.01–25	0.870	0.014
Parathion	$y = 22.096x + 52.976$	0.971	0.1–50	0.733	0.011
Chlorpyrifos	$y = 23.283x + 30.976$	0.968	0.1–50	6.563	0.126

LOD: limit of detection.

3. Results and discussion

3.1. Fluorescence intensity of cross-reaction between fluorescent markers

We investigated FAM, Cy3, and Cy5 as fluorescent labels and measured their fluorescence signals at specific wavelengths. As shown in Fig. 1, these fluorophores had the highest fluorescence intensity at Ex 460 nm/Em 520 nm, Ex 532 nm/Em 568 nm, and Ex 640 nm/Em 675 nm, respectively, and their mutual influence was negligible. Hence, FAM, Cy3, and Cy5 were selected as labels on the RNA strand for the detection method.

3.2. Optimization of monoclonal antibody loading on gold nanoparticles

In this experiment, if there were few antibody labels on the colloidal gold, the antibodies would have a lower capacity to specifically bind to the coated antigen or small pesticide molecules on the 96-well plate. On the other hand, if there were too many antibodies, the colloidal gold might also be labeled. If the antibody occupied the colloidal gold, it would lower its affinity to the ssDNA chain, thereby reducing the sensitivity of the reaction. We optimized the preparation of colloidal gold probe and triazophos, parathion, and chlorpyrifos antibodies. We added 2, 4, 6, 8, 10, and 12 μL of antibodies to determine their respective optimal dosages. As shown in Fig. 2, the highest inhibition rate was observed at 4 μL for the parathion antibody. The inhibition rate decreased when the concentration was >4 μL. As the amount of chlorpyrifos antibody increased, the inhibition reaction first increased and then decreased. The inhibition rate was the highest at 8 μL, where sensitivity was also the highest. Thus, the optimal antibody dosages when preparing the colloidal gold probes were 4, 4, and 8 μL for triazophos, parathion, and chlorpyrifos, respectively.

3.3. Cross-reactivity of the assay system

While specific binding of antigen and antibody is a prerequisite to successfully developing immunoassays for multi-residue detection, particular hybridization of complementary DNA and RNA plays a vital role. The pesticide concentration could be too high or too low if the antibody cannot recognize the corresponding antigen in a mixed hapten system. If ssDNA and RNA cannot be hybridized according to the complementary base pairing rule, the hybrid strand cannot be synthesized, and RNase H cannot specifically hydrolyze the RNA strands in the hybrids. Under the effect of inhibitors, the fluorescent group cannot be excited to emit fluorescence even at the appropriate wavelength, resulting in false-positive results. Based on optimization experiments, the OVA-haptens of triazophos, parathion, and chlorpyrifos were diluted 16,000, 8,000, and 8,000-fold, respectively. After dilution, the OVA-hapten concentrations of triazophos, parathion, and chlorpyrifos were 0.28, 0.95, and 0.79 μg/L, respectively. The colloidal gold nanoprobes were diluted 30-fold, and 5 ng/mL OPs was added to each group. Since this cross-reaction was explored in a multi-residue detection system, the experimental work was divided into three groups, exploring the reaction of single half antigen with single and mixed DNA probes, single and mixed RNA strands, as well as mixed haptens. The wavelengths for detecting triazophos, parathion, and chlorpyrifos were 460/520, 532/568, and 640/675, respectively. The results from the parathion group showed that the fluorescence values detected by different combinations are generally similar (Fig. 3). In contrast, triazophos and chlorpyrifos groups with mixed OVA-hapten, mixed colloidal gold nanoprobe, and mixed RNA chain displayed slightly higher fluorescence values than a combination of single OVA-hapten, single colloidal gold nanoprobe, and single RNA chain. However, the

Table 3
The experimental results of the spiked recovery ($n = 5$).

Pesticides	Samples	Spiked concentration (μg/kg)	Bio-barcode immunoassay		LC-MS/MS	
			Recovery (%)	RSD (%)	Recovery (%)	RSD (%)
Triazophos	Apple	10	104.4	13.9	92.6	4.66
		50	92.1	9.8	109.0	2.23
		100	97.1	11.1	96.2	3.26
	Orange	10	96.3	13.7	104.0	6.22
		50	86.4	8.62	104.0	3.71
		100	92.5	10.4	101.0	6.98
	Pear	10	100.7	12.6	105.0	6.70
		50	87.6	7.6	109.0	3.02
		100	99.0	8.4	79.4	4.29
	Cabbage	10	109.1	15.6	98.0	5.13
		50	101.2	11.7	109.0	3.87
		100	91.4	7.5	104.0	3.17
	Rice	10	105.8	10.4	89.0	8.80
		50	96.1	9.4	94.4	9.62
		100	86.3	12.2	87.4	4.35
Parathion	Apple	10	88.4	9.7	92.6	8.70
		50	80.6	8.4	95.8	2.50
		100	93.7	8.4	90.3	1.90
	Orange	10	82.4	14.4	89.4	3.60
		50	80.3	7.3	92.5	5.40
		100	81.4	8.5	101.9	2.76
	Pear	10	83.7	13.5	90.4	7.81
		50	86.6	15.2	93.1	6.69
		100	83.2	7.4	89.7	5.36
	Cabbage	10	86.2	17.6	95.8	4.68
		50	80.3	9.0	95.6	4.17
		100	88.5	9.2	93.7	2.31
	Rice	10	84.6	15.5	96.1	8.45
		50	82.0	11.0	98.3	1.92
		100	87.1	8.6	89.2	3.68
Chlorpyrifos	Apple	10	94.4	16.0	90.0	3.34
		50	102.1	10.9	97.9	7.76
		100	89.9	7.6	101.8	5.18
	Orange	10	99.9	12.0	90.5	4.96
		50	86.4	14.8	93.7	6.71
		100	101.4	8.9	85.4	4.23
	Pear	10	92.0	12.9	104.4	8.35
		50	87.4	7.4	90.6	6.76
		100	110.8	12.8	91.5	4.14
	Cabbage	10	84.4	11.9	101.8	3.82
		50	98.3	10.6	98.3	1.09
		100	95.6	9.2	85.7	2.97
	Rice	10	90.6	14.3	88.6	7.56
		50	95.0	8.5	99.1	8.47
		100	88.2	10.5	92.7	5.22

RSD: relative standard deviation.

Table 4
The parameters of developed calibration curves of LC-MS/MS for five samples.

Samples	Linear equation	Correlation coefficient	Linear range (μg/L)
Apple	$y = 10649.9x - 1584.32$	0.9999	0.1–100
Orange	$y = 9946.62x + 10914.8$	0.9996	0.1–100
Pear	$y = 9835.71x + 193455$	0.9998	0.1–100
Cabbage	$y = 9983.85x - 7100.03$	0.9997	0.1–100
Rice	$y = 1863.39x + 4525.71$	0.9994	0.1–100

difference was insignificant, and the cross-reactivity can be considered to be within the acceptable range and the method can be applied to pesticide multi-residue detection.

3.4. Optimization of dilution factor for OVA-hapten and colloidal gold probe in multi-residue bio-barcode immunoassay

To establish a more efficient and accurate multi-residue detection system, the optimal dilution of immunoreagents in various pesticide systems (triazophos, parathion, and chlorpyrifos) used a 10 mM PBS solution. The lower the IC_{50} value and the higher the F_{max}/IC_{50} value, the higher the sensitivity and accuracy of the experimental system. In Fig. 4, the various pesticide systems (triazophos, parathion, and chlorpyrifos) F_{max}/IC_{50} values reached the maximum. The lowest IC_{50} values (sensitivity) were obtained when triazophos OVA-hapten was diluted 16,000-fold, parathion and chlorpyrifos OVA-hapten were diluted 8,000-fold, and all three colloidal gold nanoprobes were diluted 30-fold.

3.5. Establishment of the standard curve for the multi-residue system

The stock solutions of the three pesticides were diluted to a series of concentrations from 0.01 to 50 ng/mL, using 5% methanol-PBS (0.01 mol/L) solution. Then, the experiments were carried out according to Section 2.3. The whole experimental system contains mixed OVA-hapten and pesticide. The colloidal gold nanoprobe explicitly recognizes the target OVA-hapten and pesticide small molecules. The plate wash solution did not wash away the probe bound to the OVA-hapten on top of the 96-well plate, thus remaining in the experimental system, participating in the hybridization reaction, and dissociating the fluorescent group on the RNA strand down by the action of RNase H. The fluorescence signal was detected at a specific wavelength. It is worth noting that the higher the pesticide concentration in the system, the probability of the probe binding to pesticide increases. The likelihood of binding to the OVA-hapten on the well plate decreases, resulting in a lower value of the detected fluorescence signal. The final detected fluorescence value in the experimental system was negatively correlated with the pesticide concentration. The standard curve is plotted using the log value of the pesticide concentration as the horizontal coordinate and the fluorescence inhibition rate as the vertical coordinate. From Table 2, it can be seen that the three pesticides, namely, triazophos, parathion, and chlorpyrifos, showed good linearity in the ranges of 0.01–25, 0.1–50, and 0.1–50 ng/mL, respectively. The established method showed a sensitivity of 0.870 ng/mL and LOD of 0.014 ng/mL for triazophos. The sensitivity for parathion was 0.733 ng/mL, with the LOD of 0.011 ng/mL, and the sensitivity for chlorpyrifos was 6.563 ng/mL, with the LOD of 0.126 ng/mL.

In summary, the established DNA/RNA hybridization-based multi-residue bioassay method could simultaneously detect the residues of the three pesticides in the range of 0.011–0.126 ng/mL. It could achieve the accurate detection of multiple pesticides with high sensitivity.

3.6. Spiked recovery experiment

To verify the accuracy of the DNA/RNA hybridization-based biological barcode method for detecting OPs in agricultural products, apples, oranges, pears, cabbages, and rice were purchased from local farmers' markets and checked to be free from pesticide residues by LC-MS/MS. The samples were processed according to Section 2.6. The mixed standard solutions of the

Table 5
Comparation between the developed method and other immunoassays.

Method	Pesticide	Spiked samples	Recovery (%)	RSD (%)	Linear range (ng/mL)	LOD (ng/mL)	IC_{50} (ng/mL)	Refs.
CFBBCIA	Triazophos	Water, rice, cucumber, apple, and cabbage	96.1	12.3	0.01–20	0.006	–	[33]
LFIC	Parathion, parathion-methyl, and fenitrothion	Cucumber, tomato, and orange	67–120	≤19.54	0.98–250	–	3.44, 3.98, 12.49	[34]
CCLEIA	Triazophos	Lettuce, apple, carrot, water, and soil	100.7	19.8	0.04–5	0.063	0.87	[35]
BI	Trichlorfon and chlorpyrifos	Orange and carrot	77.8–92.0	≤4.0	1–100000	18.0, 19.0	11000, 9000	[36]
FPIA	Parathion, phoxim, coumaphos, quinalphos, and triazophos	Water, cowpea, and leek	103.1	10.1	16.09–512	5.860	–	[37]
ELISA	Paraoxon-ethyl, fenamiphos, triazophos profenofos, and acephate	Cabbage and lettuce	85.8–105.5	≤10.4	–	13.0, 24.0, 118, 27.0, 163	354, 527, 2218, 675, 261	[38]
BA-IA	Triazophos, carbofuran, and chlorpyrifos	Cabbage, carrot, and spinach	84.5	12.3	0.02–50, 0.5–500, 1.0–1000	0.024, 0.93, 1.68	–	[39]
CLEIA	Parathion, parathion-methyl, and fenitrothion	Apple, Chinese cucumber, and rice	73–118	3.35–10.12	0.39–100, 0.10–25, 0.10–25	–	5.43, 1,34, 1.24	[40]
BBC-IA	Triazophos	Apple, cabbage, orange, and rice	89.5	15.5	0.04–10	0.020	–	[41]
CIA-BBC	Triazophos	Apple, cabbage, orange, and rice	92.1	14.0	0.015–4	0.014	–	[42]
CFAQIA-BBC	Triazophos, parathion, and chlorpyrifos	Apple, cucumber, cabbage, pear, and orange	80.3–110.8	7.3–17.6	0.01–25, 0.1–50, 0.1–50	0.014, 0.011, 0.126	0.870, 0.733, 6.563	This work

–: no data. CFBBCIA: competitive fluorescence bio-barcode immunoassay; LFIC: lateral flow immunochromatographic assay; CCLEIA: competitive chemiluminescent enzyme immunoassay; BI: biomimetic iImmunoassay; FPIA: fluorescent polarization immunoassay; ELISA: enzyme-linked immunosorbent assays; BA-IA: bead-array competitive immunoassay; CLEIA: chemiluminescence enzyme immunoassay; BBC-IA: bio-barcode amplification immunoassay; CIA-BBC: colorimetric immunoassay based on bio-barcode; CFAQIA-BBC: competitive fluorescence anti-quenching immunoassay based on bio-barcode.

three OPs (triazophos, parathion, and chlorpyrifos) were diluted with 5% methanol-PBS solution to final concentrations of 10, 50, and 100 μg/kg, respectively. The spiked recovery experiments were performed using the established method and LC-MS/MS. The results in Table 3 show that the spiked recoveries obtained using the established method ranged from 80.3% to 110.8%, with relative standard deviation (RSD) values ranging from 7.3% to 17.6%. The results obtained using LC-MS/MS ranged from 79.4% to 109.0%, with RSD values ranging from 1.09% to 9.62%. The results detected by the two methods were consistent, so the developed method was highly accurate for detecting OPs in agricultural products.

3.7. Comparison with bio-barcode immunoassay based on fluorescence anti-quenching

We established a bio-barcode immunoassay based on fluorescence anti-quenching. We set an intuitive correlation with the proposed method for detecting OPs. The standard curves of LC-MS/MS for five samples are shown in Table 4. The results for detecting OP residues in apples are shown in Fig. S2. The differences between the designed method and other immunoassays in terms of linear range, detection limit, IC_{50}, spiked recovery, and RSD are summarized in Table 5 [33–42].

4. Conclusions

This study established a biological barcode multi-residue immunoassay based on DNA/RNA hybridization to simultaneously detect triazophos, parathion, and chlorpyrifos. Five agricultural products were selected for recovery to verify the accuracy of the developed method. The recovery rate obtained by the established method was 80.3%–110.8%, and the RSD value was 7.3%–17.6%. In contrast, the recovery rate and the RSD were 79.4%–109% and 1.09%–9.62% using LC-MS/MS. The results obtained by the two methods correlated well, indicating that the method has good accuracy and reliability. Therefore, this method can simultaneously quantify triazophos, parathion, and chlorpyrifos in one run.

CRediT author statement

Lingyuan Xu: Writing - Original draft preparation, Investigation, Conceptualization, Methodology; **Xiuyuan Zhang:** Conceptualization, Investigation, Methodology, Visualization; **A.M. Abd El-Aty:** Validation, Formal analysis, Writing - Reviewing and Editing; **Yuanshang Wang:** Investigation; **Zhen Cao:** Investigation; **Huiyan Jia:** Investigation; **J.-Pablo Salvador:** Validation, Writing - Reviewing and Editing; **Ahmet Hacimuftuoglu**: Investigation; **Xueyan Cui**: Investigation; **Yudan Zhang**: Investigation; **Kun Wang**: Investigation; **Yongxin She:** Investigation; **Fen Jin:** Investigation; **Lufei Zheng:** Supervision, Funding acquisition; **Baima Pujia:** Investigation; **Jing Wang:** Funding acquisition, Supervision; **Maojun Jin:** Conceptualization, Methodology, Funding acquisition, Project administration, Supervision; **Bruce D. Hammock:** Validation, Writing - Reviewing and Editing, Funding acquisition.

Declaration of competing interest

The authors declare that there are no conflicts of interest.

Acknowledgments

This work was supported by the Central Public Interest Scientific Institution Basal Research Fund for the Chinese Academy of Agricultural Sciences (Grant No.: Y2021PT05), National Institute of Environmental Health Science Superfund Research Program (Grant No.: P42 ES004699), National Academy of Sciences (Subaward No.: 2000009144), and Ningbo Innovation Project for Agro-Products Quality and Safety (Grant No.: 2019CXGC007).

Appendix A. Supplementary data

Supplementary data to this article can be found online at https://doi.org/10.1016/j.jpha.2022.05.004.

References

[1] M. Hasanuzzaman, M.A. Rahman, M.S. Islam, et al., Pesticide residues analysis in water samples of Nagarpur and Saturia Upazila, Bangladesh, Appl. Water Sci. 8 (2018) 1–6.
[2] J. Butler-Dawson, K. Galvin, P.S. Thorne, et al., Organophosphorus pesticide exposure and neurobehavioral performance in Latino children living in an orchard community, Neurotoxicology 53 (2016) 165–172.
[3] G. Briceño, H. Schalchli, A. Mutis, et al., Use of pure and mixed culture of diazinon-degrading *Streptomyces* to remove other organophosphorus pesticides, Int. Biodeterior. Biodegrad. 114 (2016) 193–201.
[4] X. Zou, X. Xiao, H. Zhou, et al., Effects of soil acidification on the toxicity of organophosphorus pesticide on *Eisenia fetida* and its mechanism, J. Hazard Mater. 539 (2018) 365–372.
[5] M. Li, X. Hua, M. Ma, et al., Detecting clothianidin residues in environmental and agricultural samples using rapid, sensitive enzyme-linked immunosorbent assay and gold immunochromatographic assay, Sci. Total Environ. 499 (2014) 1–6.
[6] S. Wang, L. Ge, L. Li, et al., Molecularly imprinted polymer grafted paper-based multi-disk micro-disk plate for chemiluminescence detection of pesticide, Biosens. Bioelectron. 50 (2013) 262–268.
[7] J.M. Hicks, Fluorescence immunoassay, Hum. Pathol. 15 (1984) 112–116.
[8] A. Khanmohammadi, A.J. Ghazizadeh, P. Hashemi, et al., An overview to electrochemical biosensors and sensors for the detection of environmental contaminants, J. Iran. Chem. Soc. 17 (2020) 2429–2447.
[9] S.M. Taha, S.A. Gadalla, Development of an efficient method for multi residue analysis of 160 pesticides in herbal plant by ethyl acetate hexane mixture with direct injection to GC-MS/MS, Talanta 174 (2017) 767–779.
[10] Y. Wang, M. Jin, G. Chen, et al., Bio-barcode detection technology and its research applications: A review, J. Adv. Res. 20 (2019) 23–32.
[11] S.I. Stoeva, J.S. Lee, C.S. Thaxton, et al., Multiplexed DNA detection with biobarcoded nanoparticle probes, Angew. Chem. Int. Ed. Engl. 45 (2006) 3303–3306.
[12] Y. Li, Y.T. Cu, D. Luo, Multiplexed detection of pathogen DNA with DNA-based fluorescence nanobarcodes, Nat. Biotechnol. 23 (2005) 885–889.
[13] X. Lin, Y. Liu, Z. Tao, et al., Nanozyme-based bio-barcode assay for high sensitive and logic-controlled specific detection of multiple DNAs, Biosens. Bioelectron. 94 (2017) 471–477.
[14] S. Lv, K. Zhang, Z.Z. Lin, et al., Novel photoelectrochemical immunosensor for disease-related protein assisted by hemin/G-quadruplex-based DNAzyme on gold nanoparticles to enhance cathodic photocurrent on *p*-$CuBi_2O_4$ semiconductor, Biosens. Bioelectron. 96 (2017) 317–323.
[15] Y. Lin, Q. Zhou, D. Tang, et al., Signal-on photoelectrochemical immunoassay for aflatoxin B_1 based on enzymatic product-etching MnO_2 nanosheets for dissociation of carbon dots, Anal. Chem. 89 (2017) 5637–5645.
[16] H. Dong, X. Meng, W. Dai, et al., Highly sensitive and selective microRNA detection based on DNA-bio-bar-code and enzyme-assisted strand cycle exponential signal amplification, Anal. Chem. 87 (2015) 4334–4340.
[17] J. Chen, Z. Jiang, J.D. Ackerman, et al., Electrochemical nanoparticle-enzyme sensors for screening bacterial contamination in drinking water, Analyst 140 (2015) 4991–4996.
[18] J. Gao, X. Huang, H. Liu, et al., Colloidal stability of gold nanoparticles modified with thiol compounds: Bioconjugation and application in cancer cell imaging, Langmuir 28 (2012) 4464–4471.
[19] T. Hu, S. Lu, C. Chen, et al., Colorimetric sandwich immunosensor for $A\beta_{(1-42)}$ based on dual antibody-modified gold nanoparticles, Sensor. Actuator. B. 243 (2017) 792–799.
[20] C.-Y. Lee, R.-J. Shiau, H.-W. Chou, et al., Combining aptamer-modified gold nanoparticles with barcode DNA sequence amplification for indirect analysis of ethanolamine, Sensor. Actuator. B. 254 (2018) 189–196.
[21] S. Parween, A. Ali, V.S. Chauhan, Non-natural amino acids containing peptide-capped gold nanoparticles for drug delivery application, ACS Appl. Mater. Interfaces 5 (2013) 6484–6493.
[22] Y. Liu, Y. Liu, M. Zhou, et al., Chemiluminescence detection of protein in capillary electrophoresis using aptamer-functionalized gold nanoparticles as biosensing platform, J. Chromatogr. A 1340 (2014) 128–133.
[23] Y. Liang, Z. Zhang, Z. Liu, et al., A highly sensitive signal-amplified gold nanoparticle-based electrochemical immunosensor for dibutyl phthalate detection, Biosens. Bioelectron. 91 (2017) 199–202.
[24] J.M. Nam, A.R. Wise, J.T. Groves, Colorimetric bio-barcode amplification assay for cytokines, Anal. Chem. 77 (2005) 6985–6988.

[25] J. Liu, Z. Guan, Z. Lv, et al., Improving sensitivity of gold nanoparticle based fluorescence quenching and colorimetric aptasensor by using water resuspended gold nanoparticle, Biosens. Bioelectron. 52 (2014) 265–270.
[26] G. Liu, X. Yang, T. Li, et al., Spectrophotometric and visual detection of the herbicide atrazine by exploiting hydrogen bond-induced aggregation of melamine-modified gold nanoparticles, Microchim. Acta 182 (2015) 1983–1989.
[27] G. Yang, H. Zhuang, H. Chen, et al., A gold nanoparticle based immunosorbent bio-barcode assay combined with real-time immuno-PCR for the detection of polychlorinated biphenyls, Sensor. Actuator. B Chem. 214 (2015) 152–158.
[28] L. Du, W. Ji, Y. Zhang, et al., An ultrasensitive detection of 17β-estradiol using a gold nanoparticle-based fluorescence immunoassay, Analyst 140 (2015) 2001–2007.
[29] D. Lin, J. Wu, F. Yan, et al., Ultrasensitive immunoassay of protein biomarker based on electrochemiluminescent quenching of quantum dots by hemin bio-bar-coded nanoparticle tags, Anal. Chem. 83 (2011) 5214–5221.
[30] C. Zhang, Z. Jiang, M. Jin, et al., Fluorescence immunoassay for multiplex detection of organophosphate pesticides in agro-products based on signal amplification of gold nanoparticles and oligonucleotides, Food Chem. 326 (2020), 126813.
[31] X. Zhang, P. Du, X. Cui, et al., A sensitive fluorometric bio-barcodes immunoassay for detection of triazophos residue in agricultural products and water samples by iterative cycles of DNA-RNA hybridization and dissociation of fluorophores by ribonuclease H, Sci. Total Environ. 717 (2020), 137268.
[32] G. Chen, M. Jin, J. Ma, et al., Competitive bio-barcode immunoassay for highly sensitive detection of parathion based on bimetallic nanozyme catalysis, J. Agric. Food Chem. 68 (2020) 660–668.
[33] C. Zhang, P. Du, Z. Jiang, et al., A simple and sensitive competitive bio-barcode immunoassay for triazophos based on multi-modified gold nanoparticles and fluorescent signal amplification, Anal. Chim. Acta 999 (2018) 123–131.
[34] R. Zou, Y. Chang, T. Zhang, et al., Up-converting nanoparticle-based immunochromatographic strip for multi-residue detection of three organophosphorus pesticides in food, Front. Chem. 7 (2019), 18.
[35] M. Jin, H. Shao, F. Jin, et al., Enhanced competitive chemiluminescent enzyme immunoassay for the trace detection of insecticide triazophos, J. Food Sci. 77 (2012) T99–T104.
[36] Q. Liu, J. Tian, M. Jiang, et al., Direct competitive biomimetic immunoassay based on quantum dot label for simultaneous determination of two pesticide residues in fruit and vegetable samples, Food Anal. Method. 11 (2018) 3015–3022.
[37] Z. Xu, Q. Wang, H. Lei, et al., A simple, rapid and high-throughput fluorescence polarization immunoassay for simultaneous detection of organophosphorus pesticides in vegetable and environmental water samples, Anal. Chim. Acta 708 (2011) 123–129.
[38] Y. Li, F. Zhao, L. Zhao, et al., Development of a broad-specificity immunoassay for determination of organophosphorus pesticides using dual-generic hapten antigens, Food Anal. Method. 8 (2015) 420–427.
[39] Y. Guo, J. Tian, C. Liang, et al., Multiplex bead-array competitive immunoassay for simultaneous detection of three pesticides in vegetables, Microchim. Acta 180 (2013) 387–395.
[40] R. Zou, Y. Liu, S. Wang, et al., Development and evaluation of chemiluminescence enzyme-linked immunoassay for residue detection of three organophosphorus pesticides, Chin. J. Pesticide Sci. 19 (2017) 37–45.
[41] P. Du, M. Jin, G. Chen, et al., A competitive bio-barcode amplification immunoassay for small molecules based on nanoparticles, Sci. Rep. 6 (2016), 38114.
[42] P. Du, M. Jin, G. Chen, et al., Competitive colorimetric triazophos immunoassay employing magnetic microspheres and multi-labeled gold nanoparticles along with enzymatic signal enhancement, Microchim. Acta 184 (2017) 3705–3712.